Li et al. BMC Plant Biology (2025) 25:319
https://doi.org/10.1186/s12870-025-06348-6

BMC Plant Biology

RESEARCH

Open Access

Expression variation of *Viola APETALA3* orthologous genes is correlated with chasmogamous and cleistogamous flower development

Qiaoxia Li[1*], Yuanyuan Zhu[1], Youlong Li[1], Chenlong Chen[1], Jigang Li[1], Kun Sun[1] and Chaoying He[2,3,4*]

Abstract

Background *Viola philippica* and *V. prionantha* develop chasmogamous (CH) flowers under ≤ 12-h daylight conditions and cleistogamous (CL) flowers under long daylight (> 12-h daylight) conditions (LD), whereas *V. cornuta* develops CH flowers regardless of the daylight conditions. *APETALA3* (*AP3*) is a major floral B-function gene that regulates the organ identity and development of stamens and petals. Evolutionary changes in *AP3* orthologous genes might involve in the dimorphic flower formation. In the present study, we compared *AP3* orthologous genes among three *Viola* species.

Results The AP3 sequences were highly conserved, and obligate AP3-PISTILLATA heterodimers were universally formed. However, the floral expression of *VphAP3* in *V. philippica* and *VprAP3* in *V. prionantha* changed in response to the photoperiod. Their expression was significantly higher under 12-h daylight conditions than under 16-h daylight conditions. In contrast, *VcoAP3* expression in the floral buds of *V. cornuta* was comparable among photoperiods. In accordance with these variations in expression, correlated sequence divergences were observed in the putative regulatory regions of *Viola AP3* orthologous genes.

Conclusions Developmental inhibition of petals and stamens may result from *AP3* downregulation by LD, which thereby induces CL flowers. Our study provides insight into the molecular basis underlying the developmental evolution of environmentally dependent mating systems in dimorphic CL plants.

Keywords *APETALA3*, Chasmogamous flower, Cleistogamy, Differential expression, Photoperiod, *Viola*

*Correspondence:
Qiaoxia Li
liqiaoxia8024@nwnu.edu.cn
Chaoying He
chaoying@ibcas.ac.cn
[1] Life Science College, Northwest Normal University, Anning East Road 967, Anning, Lanzhou, Gansu 730070, China
[2] State Key Laboratory of Plant Diversity and Specialty Crops / State Key Laboratory of Systematic and Evolutionary Botany, Institute of Botany, Chinese Academy of Sciences, Nanxincun 20, Xiangshan, Beijing 100093, China
[3] China National Botanical Garden, Beijing 100093, China
[4] College of Life Sciences, University of Chinese Academy of Sciences, Beijing 100049, China

Introduction

Dimorphic cleistogamy is a specialized form of a mixed mating system in which a single plant produces potentially outcrossed chasmogamous (CH) and obligately self-pollinated cleistogamous (CL) flowers. CH flowers have bright, colorful petals and nectaries and remain open for cross-pollination, while CL flowers remain closed for self-fertilization [1]. Nectar and odor are absent in CL flowers, petals are rudimentary or completely missing, and stamens are often reduced in both number and size [2, 3]. The mixed mating system has important significance in the adaptive evolution of plants. CH flowers are advantageous in that they promote outcrossing and gene flow within and among populations and produce genetically diverse progenies, thus maintaining genetic diversity and adapting to the changing environment. CL flowers may be energetically less costly to produce, resulting in more available resources for seed production and extending the reproductive window of CH/CL species in adverse or extreme environmental conditions [4, 5]. A CL flower is a structurally modified form of a CH flower for autogamy and is an ecological innovation characteristic of plant adaptation to the environment [6, 7].

The floral ABC model explains how three major function class genes (A, B, and C class) determine the identity of the four floral organ types. B-class MADS-box genes in *Arabidopsis* include *APETALA3 (AP3)* and *PISTILLATA* (*PI*) [8, 9]. B-class MADS-box genes are involved not only in the specification of the organ identity of petals and stamens but also in the control of organ maturation [2, 10–12]. Mutations in either the *AP3* or *PI* genes result in similar phenotypic variations, wherein petals are transformed into sepals and stamens into carpels [10, 13, 14]. In *Arabidopsis* flowers, *AP3/PI* knockdown at intermediate stages (stages 8–10) induces petal-to-sepal transformations that gradually occur in consecutive buds, but stamens in these flowers retain their identity, become increasingly underdeveloped, and do not dehisce pollen [15]. Changes in the expression level or expression pattern of B-class MADS-box genes can create new traits and defects in floral organs [16–19]. The differential expression of the *AP3* gene is regulated by some upstream genes or environmental factors, such as the photoperiod [2, 3]. The upstream genes include *GIBBERELLIN INSENSITIVE* [20], *LEAFY*, *UNUSUAL FLORAL ORGANS* [21], *AINTEGUMENTA*, and *AINTEGUMENTALIKE6* [22]. Moreover, AP3 regulates other genes that regulate petal and stamen development [15, 23–25]. AP3 and PI positively regulate *SPOROCYTELESS/NOZZLE* expression, which is required during the late stages of stamen development in *Arabidopsis* for microsporogenesis and consequent pollen formation [15, 26]. FaesAP3_1 regulates the *FaesELF3* gene, which determines the filament length of long-homostyle *Fagopyrum esculentum* [25]. In addition, B-class genes *AP3* and *PI* and C-class gene *AGAMOUS* (*AG*) act redundantly with each other and in combination with *SEPALLATA* genes to activate *CRABS CLAW* in nectaries and carpels [23]. Transcription factor complex CmAP3-CmPI-CmUIF1 modulates carotenoid metabolism by directly regulating the carotenoid cleavage dioxygenase gene *CmCCD4a-2* in *Chrysanthemum* flowers [24]. The organ alterations of these molecular interactions resemble the floral organ variations in sizes and numbers of petals and stamens during the CH–CL transition.

The *Viola* genus (true violets) is well known for its large number of species displaying a CH/CL mixed breeding system [2, 3, 27, 28]. *Viola philippica* and *V. prionantha* possess significant and unique efficacy in clinical antiviral therapy. *Viola philippica* and *V. prionantha* extract from whole plants possess a wide range of pharmacological and biological activities, including antiviral, antifungal, anticoagulant, and anticancer functions [29–31]. Photoperiods play an important role in the development of CH and CL flowers in *Viola*, such as *Viola philippica*, *V. prionantha*, and *V. odorata* [2, 3, 27]. In *Viola*, CH flowers are fully developed and typically feature large, showy petals, while CL flowers have reduced stamens and undeveloped petals [2, 3, 27, 28]. CH and CL flowers are developed on the same individual plants at the different times of the season in *Viola*, and intermediate cleistogamous (inCL) flowers are occasionally developed under 12-h daylight conditions, which display variable characteristics, with poorly or less developed petals and stamens [2, 3]. In *V. philippica* and *V. prionantha*, CH flowers are induced under short-day or intermediate daylight conditions, and photoperiod extension is intended to induce CL flower formation [2, 3]. But, the *V. cornuta* CH flower type is not changed under varying photoperiod conditions (> 10 h of daylight), nonetheless, it hardly blooms under short (≤ 10-h) daylight conditions. The variation in the expression of the B-class MADS-box genes *TOMATO MADS BOX GENE 6* (*TM6*) and *PI* during CH–CL development has been observed in *V. philippica* [2]. *AP3* is the paralogous gene of *TM6* [32]. These homologous genes are partially redundant and play a role in the diversification of floral morphology during evolution [33]. However, whether photoperiod regulates the expression of *AP3* in *Viola*, and its implication in the CH–CL transition remain unknown. The aims of this study were to isolate the open reading frame (ORF), gDNA, and promoter of *AP3* orthologous genes in three *Viola* species to investigate their sequence conservation and divergence, protein–protein interactions (PPIs), and mRNA expression levels and to show their potential roles in the CH–CL transition. This work provides additional evidence for the involvement of floral B-class genes in the developmental evolution of dimorphic flower in *Viola*.

Materials and methods

Plant materials and growth conditions

Seeds of *V. philippica*, *V. prionantha*, and *V. cornuta* were collected on the Northwest Normal University (Lanzhou, Gansu, China) campus. The plants were grown at 22–26 °C under 12 or 16 h of daylight in growth chambers. The procedures and conditions for plant cultivation followed the previous description by Li et al. [2].

Flower morphology observation

The morphology of *V. philippica*, *V. prionantha*, and *V. cornuta* flower buds was observed under a stereomicroscope (Olympus SZ61, Tokyo, Japan). Mature flowers of each type (CH and CL) were analyzed. Images were captured using a camera (Olympus, DP20-DRV, Tokyo, Japan) linked to a stereomicroscope (Olympus SZ61, Tokyo, Japan).

Sequence isolation

The cDNA fragments of the targeted genes were isolated using specific primers (Table S1) designed based on the full-length transcriptome data from *V. prionantha* [3]. The full-length cDNA was assembled according to the previous description by Li et al. [2].

Phylogenetic analysis

The amino acid sequences of these genes were aligned using CLUSTALW2.0 [34] with default settings and manual adjustments. Gaps were introduced for proper alignment. A maximum likelihood phylogeny tree based on amino acid sequences was constructed [35]. Bootstrap values were based on 1000 replicates.

Quantitative reverse transcription-polymerase chain reaction (qRT-PCR)

According to naked-eye observations of the floral buds, CH and CL flower buds from stages 1, 2, 3, 4, and 5 (also defined as F1, F2, F3, F4, and F5) [3] and floral organs from stage 5 (F5) were collected under 12- and 16-h light periods. Total RNA was extracted using TRIzol reagent (TIANGEN, Beijing, China). qRT-PCR was performed using a PrimeScript RT Reagent Kit (TaKaRa, Dalian, China), SYBR Premix EX Taq II (TaKaRa, Dalian, China), and gene-specific primers (Table S1). An 18S ribosomal RNA gene was used as an internal reference (AB354544.1). The amplification conditions were same as the previous study [2]. Expression levels were calculated according to a previous description [36].

RNA *in situ* hybridization

Floral buds at different developmental stages were fixed in 4% (wt/vol = 4 g/100 mL) paraformaldehyde and embedded in Paraplast (Sigma P3683, St. Louis, MO, USA). When ATG was set as 1, a 300-bp fragment of *VphAP3* (positions 397–696), *VprAP3* (positions 397–696), and *VcoAP3* (positions 394–693) were used as templates for both sense and antisense probe synthesis using the DIG RNA labeling kit (Roche, Mannheim, Germany) and T7 RNA polymerase (Roche, Mannheim, Germany). Hybridization was performed as previously described by Javelle et al. [37]. Sections of floral tissues of CH and CL flowers from the three *Viola* species were incubated in the same hybridization solution for each probe. Images were captured with a microscope (Nexcope, Ningbo, Zhejiang, China).

Yeast two-hybrid (Y2H) analysis

The ORFs of the involved *Viola* B-class MADS-box genes were cloned into the pGADT7 or PGBKT7 vector (Clontech, Mountain View, CA, USA). The co-transformed yeast cells were selected by growth on synthetic drop-out medium (SD) plates lacking leucine (Leu) and tryptophan (Trp). Interactions were analyzed on SD plates lacking Leu, Trp, adenine (Ade), and histidine (His) and further confirmed by the non-lethal ß-galactosidase activity assay in yeast strain AH109. Before checking the PPIs, the toxicity and self-activation capability of these *Viola* B-class MADS-domain proteins were checked. Briefly, these experiments followed the previous description by Gong and He [38].

Bimolecular fluorescence complementation (BiFC) assay

A BiFC assay was conducted using *Nicotiana benthamiana* leaf cells. The ORFs of the involved *Viola* B-class MADS-box genes lacking the stop codon were cloned into the pSPYNE-35S and pSPYCE-35S vector pair using the *Xba I*/*Xho I* and *Xba I*/*Kpn I* (TaKaRa, Dalian, China) restriction sites. These paired vectors were designed to express either the N- or C-terminal halves of the yellow fluorescence protein (YFP). The construct combination of two proteins fused with the N- or C-terminal halves of YFP was agroinfiltrated into *N. benthamiana* leaf epidermal cells. After 48 h, the YFP fluorescence signals were observed using a laser confocal microscope (Leica, Wetzlar, Germany).

Promoter isolation and prediction

The *VphAP3* and *VcoAP3* genomic sequences were isolated via PCR using the KOD-Plus enzyme (Takara, Dalian, China) and gene-specific primers (Table S1). The putative promoter sequences of each gene were acquired using the Genome Walking Kit (Takara, Dalian, China) based on the obtained genomic sequences. *Cis*-element prediction was performed using PlantCARE (https://bioinformatics.psb.ugent.be/webtools/plantcare/html/).

Sequencing and statistical analyses

Construct sequencing and primer synthesis were performed by Qingke (Xian, China). The mean ± standard deviation was calculated from at least three independent replicates. Significance differences were analyzed with Duncan's test using SPASS27.0 (SPSS Inc., Chicago, IL, USA).

Results

Floral morphology of *V. philippica, V. prionantha,* and *V. cornuta*

Viola philippica and *V. prionantha* developed both CH and CL flowers under different photoperiods. CH flowers were induced under short (10 h) and intermediate daylight (12 h) conditions, whereas CL flowers were triggered under long daylight (16 h) conditions (Fig. 1A–J) [2, 3]. The inCL flowers were occasionally formed in *V. philippica* and *V. prionantha* under 12-h daylight conditions and they had 1–3 poorly developed petals and 2–5 developed stamens (Fig. 1E and J). However, *Viola cornuta* hardly bloomed under ≤ 10 h of daylight and only developed CH flowers under ≥ 10 h (12 and 16 h) of daylight, and no CL and inCL flowers were developed under any photoperiod conditions (Fig. 1K–L). The CH flowers of the three *Viola* species had five large and showy petals, with the lowest protruding at the base into a spur, and five stamens. Each stamen had four pollen sacs, and the lowest two stamens had noticeable nectar glands attached to them (Fig. 1A, B, E, F, G, K, and L). The CL flowers of *V. philippica* and *V. prionantha* had two stamens without nectar glands, each stamen had two pollen sacs, and the five petals were all undeveloped (Fig. 1C, D, H, and I). The filament of CL stamens was distinct compared with that of CH flowers, which were undetectable (Fig. 1B, D, G, and I). Thus, *V. cornuta* is a suitable control for revealing the genetic variations and mechanisms of dimorphic flower formation.

According to naked-eye observations of the floral buds, roughly five floral developmental stages (F1–F5) after floral organogenesis were defined for CH and CL formation in *V. prionantha* [3], which seemed to be conserved in other *Viola* species. At F1, CH flowers had five obvious petals and stamens, and CL flowers had two stamens, with other stamens and all petals retained as rudimentary structures (Fig. S1A–E). At F2, the nectar glands at the base of the two stamens began to appear in CH flowers. In CL flowers, the five petals and the other three stamens remained in the organ rudimentary state, and the filaments of the stamen began to appear visibly (Fig. S1F–J). At F3, the nectar glands at the base of the two stamens were obvious in CH flowers, and the stigma was higher than in the stamen. In CL flowers, the filaments of the stamen became distinct at F3 (Fig. S1K–O). At F4,

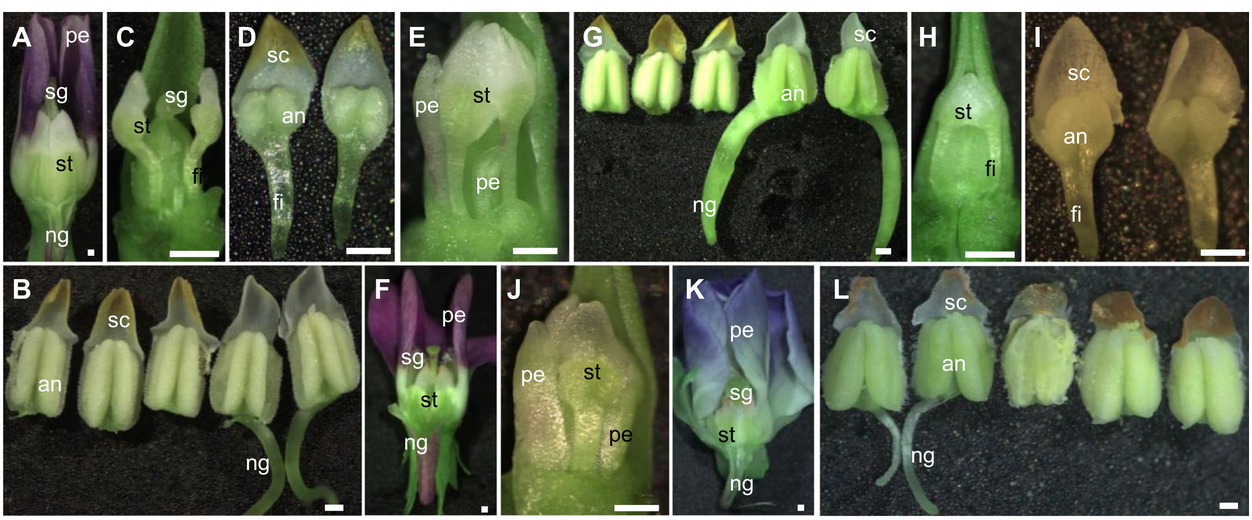

Fig. 1 Floral variations under different photoperiods in three *Viola* species. **A**–**E** *Viola philippica*. **A** Chasmogamous (CH) flower under 12-h daylight conditions. **B** Stamen of a CH flower. **C** Cleistogamous (CL) flower under 16-h daylight conditions. **D** Stamens of a CL flower. **E** Intermediate CL (inCL) flower under 12-h daylight conditions. **F**–**J** *Viola prionantha*. **F** CH flower under 12-h daylight conditions. **G** Stamen of a CH flower. **H** CL flower under 12-h daylight conditions. **I** Stamens of a CL flower. **J** inCL flower under 12-h daylight conditions. **K**, **L** Viola cornuta. **K** Normal CH flower under 12- and 16-h daylight conditions. **L** Stamen of a CH flower. No CL and inCL flowers were developed in *V. cornuta* under 12-h daylight conditions. Bars = 500 μm in A–L. se, sepal; pe, petal; st, stamen; ca, carpel; sg, stigma; an, anther; sc, stamen cap; fi, filament; and ng, nectar gland

the petals outside the flower buds were visible and pigmented, and the stamen cap became white in CH flowers. In CL flowers, the stamen cap also became white, and the development of the three stamens and all petals was completely arrested as primordial structures (Fig. S1P–T). At F5, in CH flowers, the petals turned purple, and the stamen cap became yellow. In CL flowers, the stamen cap also became yellow, and the development of the three stamens and all petals was completely arrested as primordial structures (Fig. S1U–Y).

Sequencing analysis of AP3 orthologous genes in three Viola species

Using the full-length transcriptome data of *V. prionantha* and RACE, we acquired the cDNA of the *AP3* lineages of the MADS-box genes from *V. philippica*, *V. prionantha*, and *V. cornuta*. The ORFs of *VphAP3*, *VprAP3*, and *VcoAP3* were 696, 696, and 693 bp in length, putatively encoded polypeptides of 231, 231, and 230 amino acids, and had corresponding genomic regions of 1838, 1844, and 1552 bp in length, respectively. A maximum likelihood (ML) phylogenetic tree showed that the AP3 lineage proteins of the three *Viola* species clustered and that these AP3 lineage proteins were grouped with previously reported AP3-like proteins, such as closely homologous proteins from *Arabidopsis* (Fig. 2A). Multiple sequence alignment of these genes and representatives of previously functionally inferred AP3-like proteins showed that these hypothetical AP3 proteins had a euAP3 motif at the C-terminal end (Fig. 2B), clearly confirming that these isolated sequences were orthologous to *AP3*. The sequencing identity of *Viola* AP3 orthologous genes was 95.4–98.7% among *VphAP3*, *VprAP3*, and *VcoAP3* (Fig. S2), indicating that they were highly conserved and implying the conserved biochemical functions of these *Viola* AP3 orthologs and hence a conserved developmental role.

Heterodimerization of B-class MADS-box transcription factors

B-function MADS-box genes perform essential roles in flower development by forming obligate AP3-PI heterodimers [39, 40]. We then investigated protein–protein interactions (PPIs) among these *Viola* B-class MADS-domain proteins. In a yeast GAL4 two-hybrid system (Y2H), activating both *His*3 and *LacZ* reporters enabled cell growth of the transformed yeast and generated the blue coloration in the non-lethal ß-galactosidase assay, demonstrating PPIs. No toxicity or self-activation of these proteins was observed in yeast (Fig. S3) [2]. All B-class proteins from *Viola* formed AP3-PI, TM6-PI, and AP3-TM6 heterodimers, while no homodimers were formed in yeast (Fig. 3A and B; Fig. S4). In the BiFC assay, in vivo interactions occurred between the B-class MADS-domain proteins from the examined plant species (Fig. 3C–T; Fig. S5), thus confirming the observed PPIs. These results suggest the functional conversation of these *Viola* B-class MADS-domain proteins.

Floral expression levels of Viola AP3 orthologous genes in response to photoperiod

The potential role of *AP3* in the formation of dimorphic flowers may be attributed to expression variation. CH and CL flower buds were respectively developed under 10 (12)-h and 16-h daylight conditions for *V. philippica* and *V. prionantha*, while *V. cornuta* exhibited minimal blooming under 10-h daylight conditions. To reveal the *AP3* expression variation in the CH–CL transition of *V. philippica*, *V. prionantha*, and *V. cornuta* in response to the photoperiod, the CH and CL flower buds under 12-h and 16-h daylight conditions of *V. philippica* and *V. prionantha* and the CH flower buds of *V. cornuta* that corresponded to two photoperiods (12- and 16-h daylight conditions) were selected for the expression study. We determined that the expression levels of *VphAP3* and *VprAP3* were significantly higher in CH floral buds subjected to 12-h daylight than in CL floral buds subjected to 16-h daylight, especially at the F1–F3 stage (Fig. 4A and B), thereby implying that the expression level of *VphAP3* and *VprAP3 in V. philippica* and *V. prionantha* decreased as the duration of daylight was extended. However, *VcoAP3* expression in the CH floral buds of *V. cornuta* under 12-h daylight conditions was comparable to CH floral buds under 16-h daylight conditions (Fig. 4C). These results indicate that the expression of *VphAP3* and *VprAP3* may be regulated by photoperiod and correlate to CH and CL formation in these *Viola* species.

Temporal and spatial expression of Viola AP3 genes during flower development

The spatial and temporal expression patterns of *AP3* were determined during flower development using in situ hybridization in three plant species. *VphAP3*, *VprAP3*, and *VcoAP3* in *V. philippica*, *V. prionantha*, and *V. cornuta*, respectively, were continuously expressed during flower development. They were mainly expressed in petals, stamens, and carpels (Fig. 5). *VphAP3* and *VprAP3* were expressed in the developed petals and stamens of CH flowers under 12-h daylight conditions or CL flowers under 16-h daylight conditions (Fig. 5A–H). The *AP3* expression in the undeveloped, rudimentary petals of CL flower buds was not demonstrated, although we assumed its expression in petal organs since the petal primordia is initiated [2]. In *V. cornuta*, the expression pattern of *VcoAP3* was the same in normal CH flowers under 12- and 16-h daylight

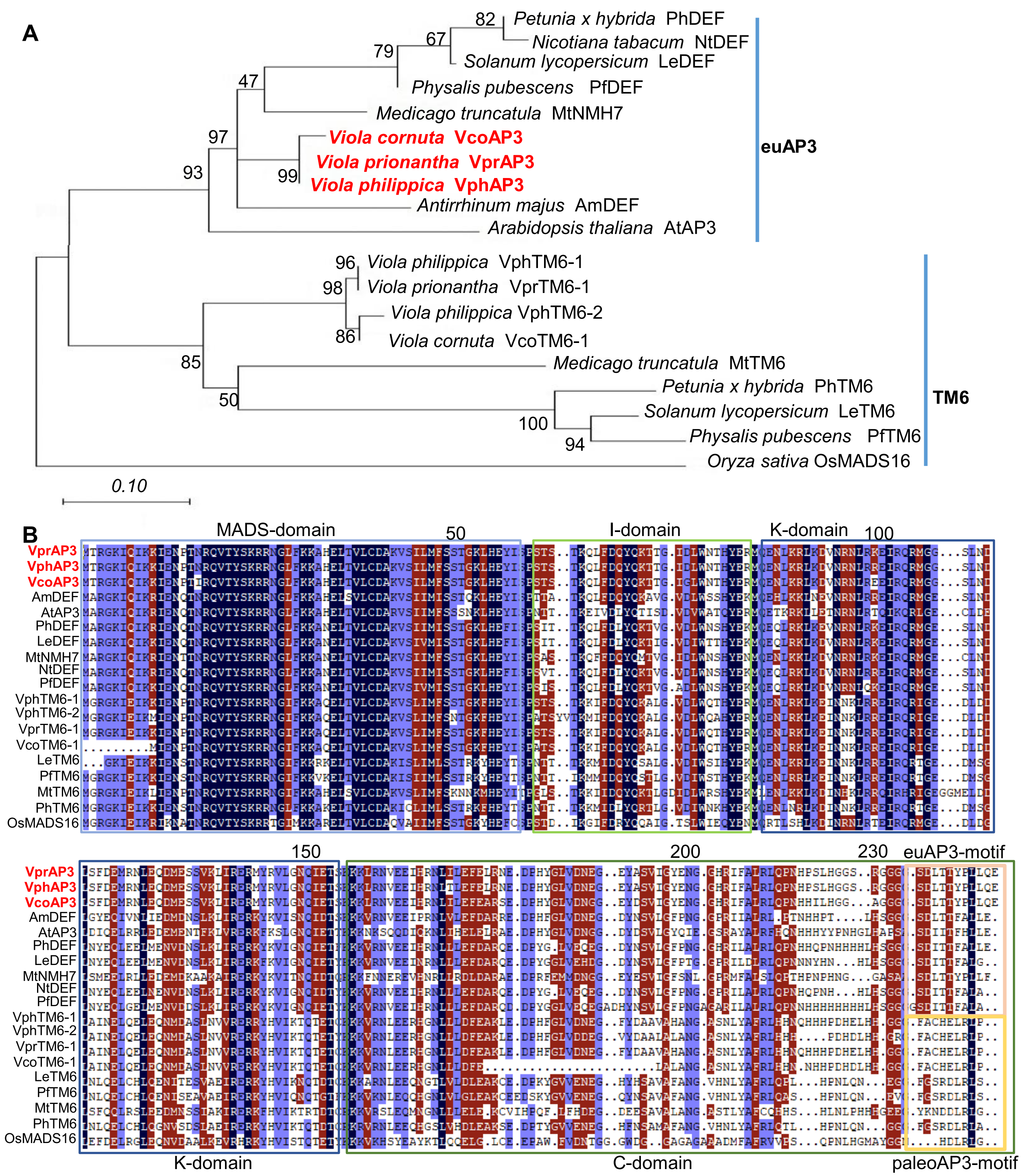

Fig. 2 Sequence characterization of AP3 in *Viola*. **A** Maximum Likelihood (ML) tree of AP3-like proteins. VphAP3, VprAP3, and VcoAP3 are in red. The accession numbers of other sequences used are VphAP3 (in this study), VprAP3 (in this study), VcoAP3 (in this study), VphTM6-1 (KU318322), VphTM6-2 (KU318323), VprTM6-1 (in this study), VcoTM6-1 (in this study), LeTM6 (X60759.1), LeAP3 (DQ674532.1), PhTM6 (AF230704.1), PhDEF (X69946.1), MtTM6 (JN412097.1), MtNMH7 (JN412096.1), AtAP3 (NM115294.5), AmDEF (AB516402.1), NtDEF (X96428.1), PfDEF (KC174703.1), and PfTM6 (KC174704.1). OsMADS16 (AF077760.1) was used as the outgroup. The species name is listed before the gene name. The numbers next to the nodes are bootstrap values. **B** Multiple sequence alignment. Gaps are introduced for proper alignment. The M, I, K, and C domains of each MADS-domain protein are indicated by the light blue box, the green box, the dark blue box, and the orange box, respectively. The pink and purple boxes at the end of C-domain respectively indicate the euAP3 and paleoAP3 motifs

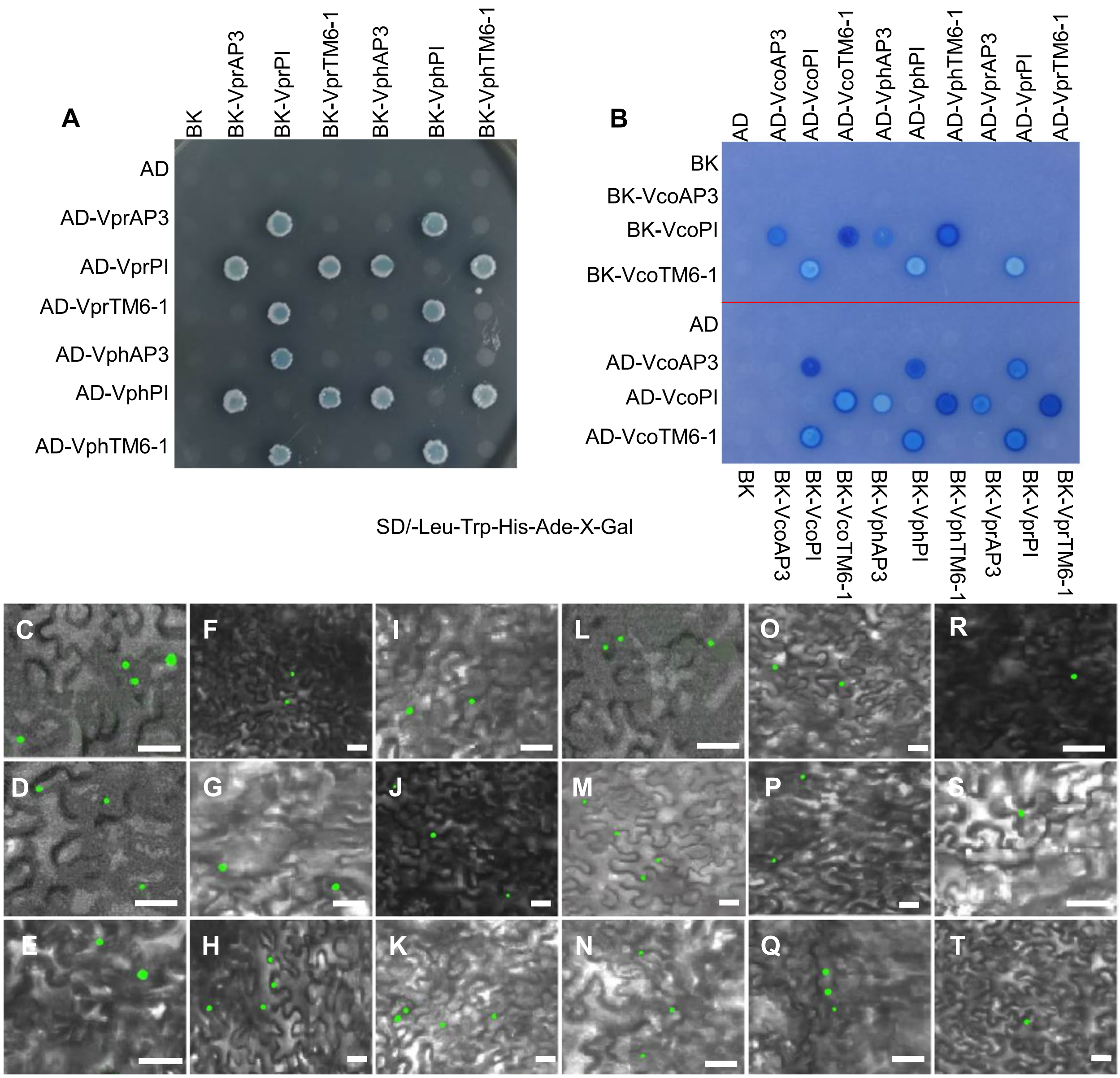

Fig. 3 Protein–protein interactions (PPIs) of B-class MADS-box transcription factors among *Viola philippica*, *V. prionantha*,and *V. cornuta*. **A**, **B** Yeast-two hybrid assays showing PPIs of AP3 and other B-class MADS-box transcription factors in the indicated *Viola* species. **C**–**T** PPIs revealed by BiFC. **C** YCE-VphAP3:YNE-VphPI; **D** YCE-VphAP3:YNE-VprPI; **E** YCE-VphAP3:YNE-VcoPI; **F** YNE-VprAP3:YCE-VphPI; **G** YNE-VprAP3:YCE-VprPI; **H** YNE-VprAP3:YCE-VcoPI; **I** YNE-VcoAP3: YCE-VphPI; **J** YNE-VcoAP3:YCE-VprPI; **K** YNE-VcoAP3:YCE-VcoPI; **L** YCE-VphTM6-1:YNE- VprPI; **M** YCE-VphTM6-1:YNE-VcoPI; **N** YNE-VphTM6-1:YCE-VphPI; **O** YNE-VprTM6-1:YCE-VphPI; **P** YNE-VprTM6-1:YCE-VprPI; **Q** YNE-VprTM6-1:YCE-VcoPI; **R** YCE-VcoTM6-1:YNE-VphPI; **S** YCE-VcoTM6-1:YNE-VprPI; and **T** YNE-VcoTM6-1:YCE-VcoPI. Bars = 50 μm

conditions, and this gene was mainly expressed in petals, stamens, and carpels (F ig. 5I–L). Furthermore, at the more mature development stage of floral buds in three species, the expression of three *Viola AP3* orthologous genes in stamens was mainly observed in anthers and less in filaments and stamen caps (Fig. 5B, D, F, H, J, and L). However, the expression levels of *VphAP3* and *VprAP3* seemed to be higher in CH flower stamens than in CL flower stamens (Fig. 5N and O), and little difference was observed in *VcoAP3* expression in the developed petals and stamens of flowers under both 12- and 16-h daylight conditions (Fig. 5P).

Taken together, inhibition of petal and stamen development in the CL flowers of *Viola* might result from the downregulation of *AP3* under long daylight conditions, suggesting that the expression variation in *AP3*

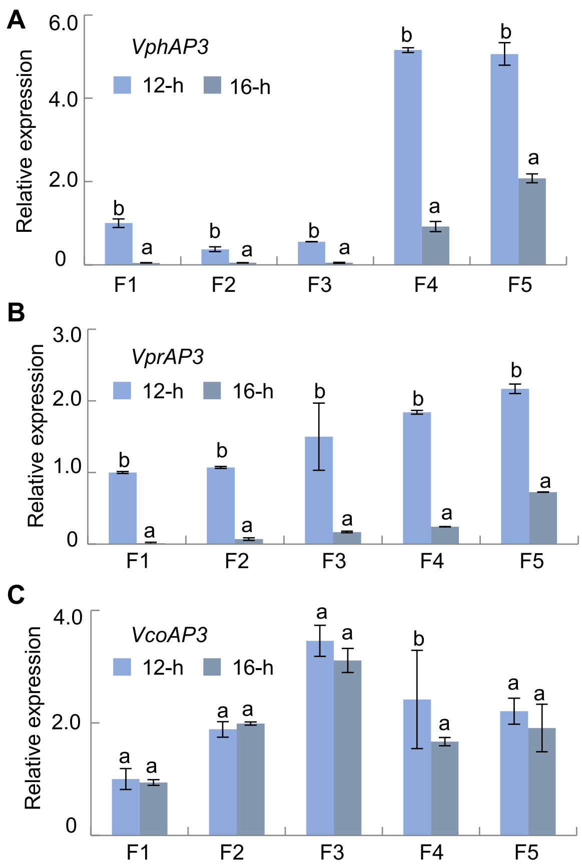

Fig. 4 Floral expression of *AP3* in response to photoperiod variation among *Viola philippica*, *V. prionantha*, and *V. cornuta*. **A** Expression of *VphAP3* under 12- and 16-h daylight conditions. **B** *VprAP3* expression under 12- and 16-h daylight conditions. **C** *VcoAP3* expression under 12- and 16-h daylight conditions. Gene expression in flower buds around F1, F2, F3, F4, and F5 under 12- and 16-h daylight conditions. Gene expression in F1 under 12-h daylight conditions was set to 1. Three independent biological samples were used in the analyses. Means and standard deviation are presented. Different lowercase letters indicate a significant difference, and the same lowercase letters indicate no significant difference

may play an essential role in the CH–CL transition of *Viola* species.

Promoter divergence of Viola AP3 may account for the differential expression

The gene structure was highly conserved (Fig. 6); therefore, the differential expression of *AP3* in the three *Viola* species may be due to differences in the regulatory sequences. The upstream sequences of the ATG of *VphAP3* and *VcoAP3*, as the putative promoter, were isolated using the genome walking method, and the length of the obtained sequences was 2822 and 2693 bp, respectively. In *V. prionantha*, the putative promoter of *VprAP3* (2754 bp) was previously cloned [3]. Sequence comparison showed that the putative promoters could be roughly divided into three regions: the *VphAP3-VprAP3-VcoAP3* conserved region (P1, − 1 to − 358 bp), the *VphAP3-VprAP3* conserved region (P2, − 359 to − 1152 bp) relative to *VcoAP3*, and the variable region (P3, beyond − 1153 bp) among the three promoters (Fig. S6). In the P1 region, the three promoters shared more than 80% sequence identity. Beyond this three-gene conserved region, *VphAP3* and *VprAP3* further remained relatively conserved (80% sequence identity) in the P2 region, but they were different from that of *VcoAP3*, sharing approximately 52% sequence identity with *VphAP3* and *VprAP3*. However, the further distal promoter sequences of *VphAP3*, *VprAP3*, and *VcoAP3* in the P3 region were quite variable and different, and the sequence identity among them was less than 42% (Fig. S6). Therefore, the *VcoAP3* promoter sequence deviated from the other two overall (*VphAP3–VprAP3*) (Fig. 6; Fig. S6). This might form a basis for the differential expression of these *Viola AP3* orthologous genes in response to photoperiod variation.

To further endorse this presumption, we further predicted the *cis*-elements on these putative promoters. Many *cis*-elements, including CArG-box, ABRE, P-box, MBS, MYB, MYC, and CGTCA-motif, were distributed in these promoters across the three defined regions (P1, P2, and P3); however, some *cis*-elements were differently distributed in the putative promoters of *VphAP3–VprAP3* or *VcoAP3*, especially *cis*-elements related to light or light response (Fig. 6; Table S2). The light-responsive element Sp1-motif was found in the promoter sequences of *VphAP3* and *VprAP3* but not in the *VcoAP3* promoter, while a chs-CMA2a element, GA-motif, Gap-box, and LS7 element were present in the promoter sequences of *VcoAP3* but not in the promoters of *VphAP3* and *VprAP3*. Moreover, auxin responsiveness TGA elements were found in the promoter sequences of *VphAP3* and *VprAP3* but not in the *VcoAP3* promoter. Furthermore, the circadian elements were revealed in the promoter sequences of *VcoAP3* but not in the promoters of *VphAP3* and *VprAP3*. In addition, sequence divergence in the introns was observed, which might be involved in the regulation of gene expression. The fourth intron of *VcoAP3* was shorter than that of *VphAP3* and *VprAP3*, which had different *cis*-elements (Fig. 6, Table S3). Overall, the presence and distribution of these *cis*-motifs in the promoters and introns of these *AP3* orthologous genes might lead to the differential expression of these genes in response to the photoperiod in the three *Viola* species.

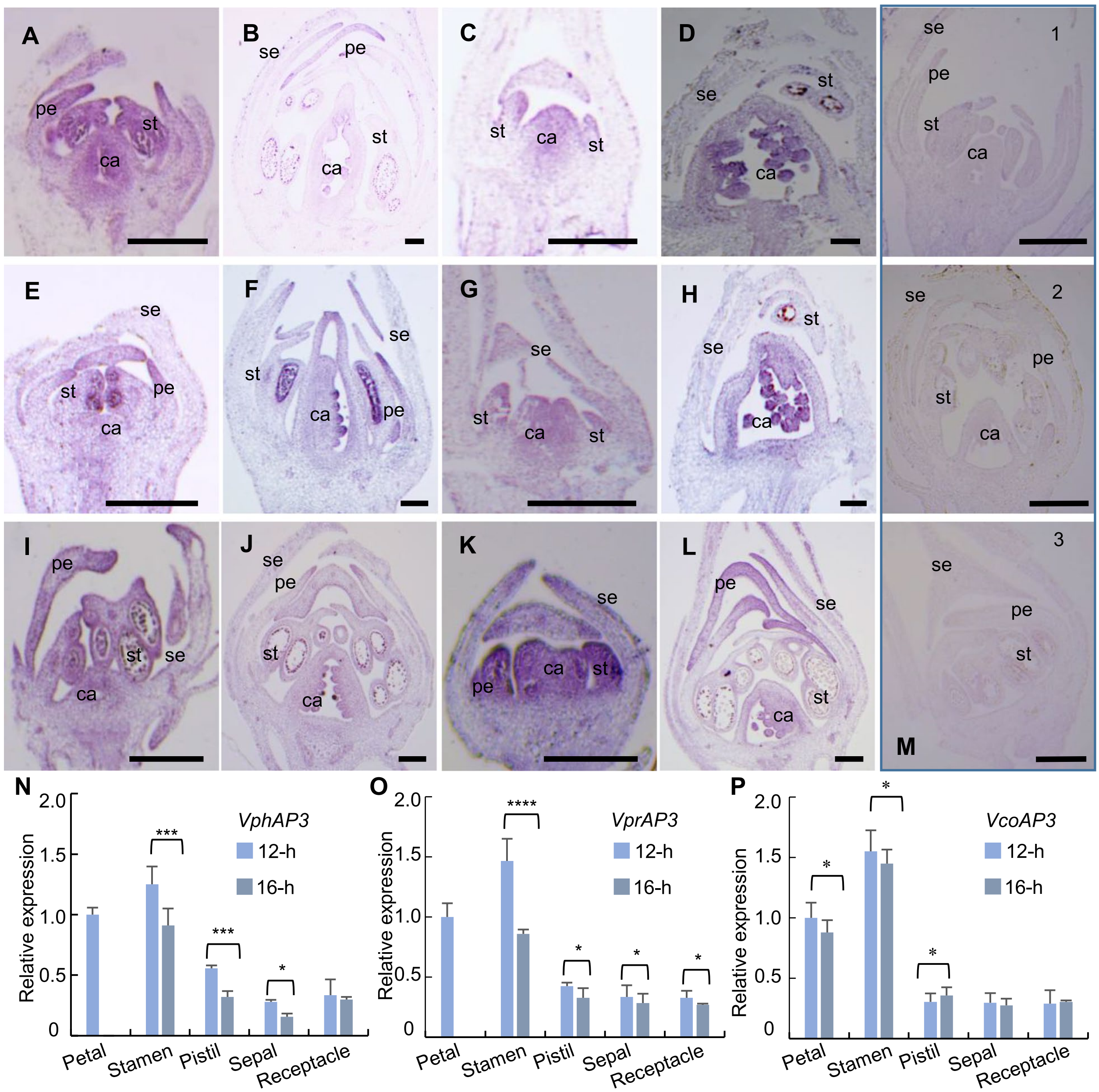

Fig. 5 Expression pattern of *AP3* orthologous genes in floral buds of *Viola philippica*, *V. prionantha*, and *V. cornuta*. **A**–**D** *VphAP3* expression at the F1 and F2 stages of (**A**, **B**) CH and (**C**, **D**) CL flowers. **E**–**H** *VprAP3* expression at the F1 and F2 stages of (**E**, **F**) CH and (**G**, **H**) CL flowers. **I**–**L** *VcoAP3* expression at the F1 and F2 stages of normal CH flowers under (**I**, **J**) 12 and (**K**, **L**) 16-h daylight conditions. The gene expression levels were determined using in situ hybridization. The developmental stages are defined as those in Fig. S1. **M** Hybridization was performed using sense probes. *VphAP3*, *VprAP3*, and *VcoAP3* are indicated by 1, 2, and 3, respectively. Bars = 100 μm. se, sepal; pe, petal; st, stamen; and ca, carpel. **N**–**P** Relative expression of (**N**) *VphAP3*, (**O**) *VprAP3*, and (**P**) *VcoAP3* in the floral organs of mature flowers. No petal sample was harvested in CL floral buds since they were undeveloped and rudimentary in *V. philippica* and *V. prionantha* under 16-h daylight conditions in N and O. The level of gene expression in the petals of CH flowers subjected to 12-h daylight conditions was set to 1. Three independent biological samples were used in all analyses. Means and standard deviation are presented. *$p < 0.05$, **$p < 0.01$, ***$p < 0.001$, and ****$p < 0.0001$ in single factor ANOVA test

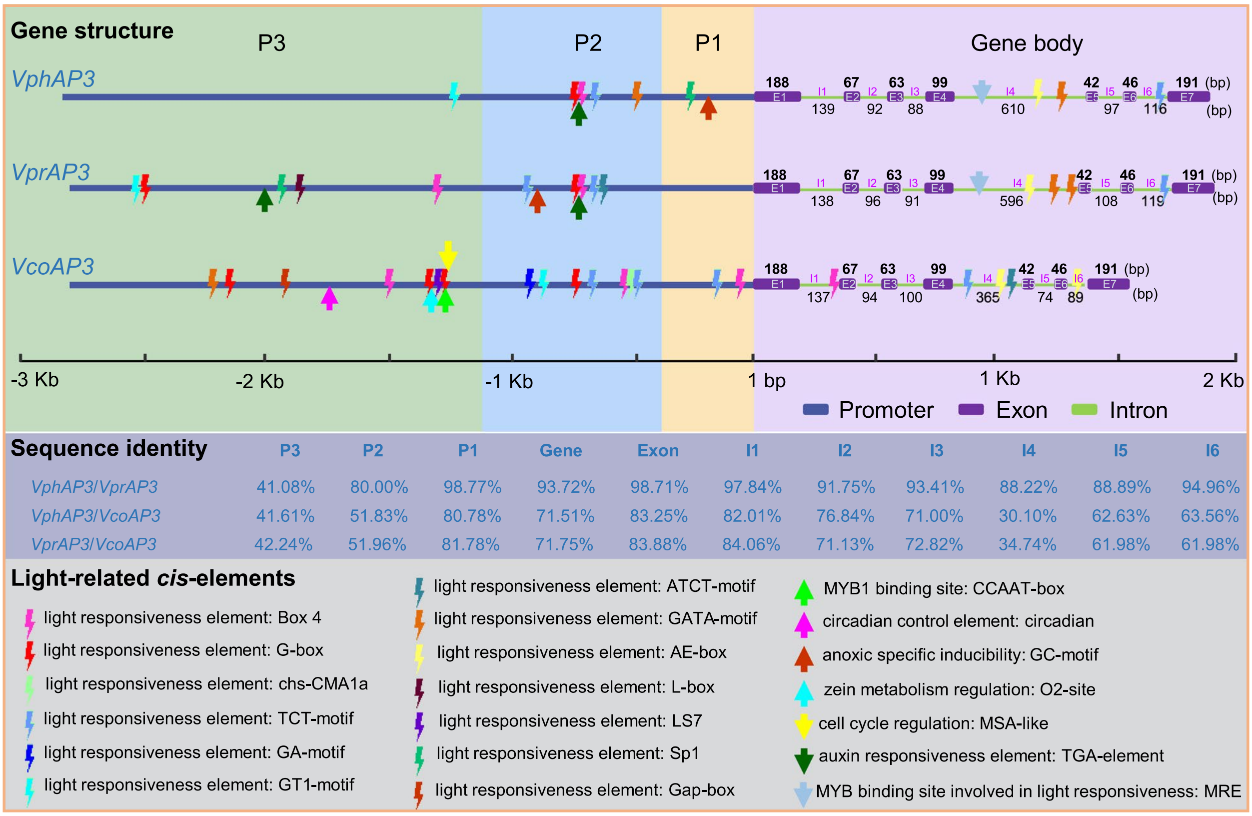

Fig. 6 Presence and distribution of *cis*-elements on the *Viola AP3* orthologous genes. The putative promoter and gene structure of *VphAP3*, *VprAP3*, and *VcoAP3* were compared. The gene structures of these *AP3* genes were conserved and included seven exons (E1–E7) and six introns (I1–I6). The three regions (P1, P2, and P3) of their putative promoters were defined according to sequence identity analyses (Fig. S6). The *cis*-elements or motifs related to light and light response are highlighted using different colored symbols, as indicated. Detailed information on these *cis*-elements is presented in Tables S2 and S3. The sequence identities of different regions of each pair of genes are given

Discussion

In dimorphic cleistogamy plants, heterogeneity in the environment may lead to phenotype selection of floral buds, and the frequencies of CH and CL flowers depend on various environmental conditions [2, 3, 27, 41–44]. The photoperiod plays a key role in CH/CL flower development in *Viola* species. CH flowers are induced under short-daylight and intermediate daylight conditions, and long-daylight (LD) induces CL flower formation in *V. philippica*, *V. prionantha*, and *Viola odorata* [2, 3, 27]. However, *V. cornuta* rarely blooms under short-daylight conditions, and normal CH flowers are always induced under intermediate daylight and LD conditions. Therefore, *V. cornuta* was a control species for elucidating the molecular mechanisms of dimorphic flower development.

From an evolutionary developmental biology perspective, alterations in coding regions or expression variation of orthologous genes may account for developmental reprogramming, thus leading to morphological variation of homologous organs between species. The main differences between CH and CL flowers lie in petal and stamen growth and morphology, which may relate to the alteration of floral B-function MADS-box genes because these genes regulate stamen and petal identity and development [10–12, 15]. Moreover, the evolution of these floral MADS-box genes and their obligate heterodimers play an important role in petal formation and diversification in core eudicots [32, 40, 45–48]. Previous work revealed that other B-function homologous genes, *VphPI* and *VphTM6*, may function in dimorphic flower formation [2]. In this study, we compared the *AP3* orthologous genes of these three *Viola* species and found that the sequences and obligate AP3-PI heterodimerization were highly conserved, indicating a high degree of conservation in biochemical and developmental roles for these *Viola AP3* orthologous genes. However, their differential expression in response to the photoperiod may contribute to the CH–CL transition in *Viola*. The changes in the expression level and pattern of *AP3-like* genes lead to innovations in flower morphology [16–19, 49–51]. The long-lasting flowers of azalea cultivars exhibit small-sized corollas during long blooming because the transcript of the *AP3* homolog was reduced [19]. Independent petal losses within the buttercup family (Ranunculaceae) are strongly associated with decreased or eliminated expression of a single floral organ identity gene, *AP3-3* [16], while petal loss in *B. frutescens* is likely associated with the lack of *AP3-3* expression and expanded *AG* expression [49]. In rice, mutants of the *AP3*-like gene *SUPERWOMAN1* have normal stamens, but their lodicules are homeotically transformed to lodicule-glume mosaic organs, thereby engendering cleistogamy [52]. Moreover, some environmental factors, such as high temperature and drought, induce *AP3* downregulation, thus leading to anther deformation and reduced male fertility [53, 54]. The differential floral expression of *PI* and *TM6* in response to variations in the photoperiod is associated with CH–CL flower development in *V. philippica* [2]. In this study, the *AP3* orthologous genes were mainly expressed in the petals, anthers of stamens, and carpels in three *Viola* species. The expression of *AP3* orthologous genes in the carpels of three *Viola* species aligns with the observations made in basal angiosperms, such as *Amborella*, *Nuphar*, and *Asarum* [55, 56]. The *AP3* and *PI* exhibited expression in the early stages of gynoecium development is likely conducive to carpel determinacy and development [57]. However, the main difference was that the expression levels of *VphAP3* and *VprAP3* in the petals and stamens of *V. philippica* and *V. prionantha* decreased as the daylight duration was extended. In contrast, the *VcoAP3* expression in *V. cornuta* under 12-h daylight conditions did not change compared with that under 16-h daylight conditions. These results indicate that the significant decrease in the expression of *AP3* orthologous genes was differentially induced by photoperiod extension, playing an essential role in CL and CH flower formation in *Viola*.

Concerning the high conservation in the coding regions and obligate AP3-PI heterodimerization, the differential expression of *AP3* orthologous genes in *V. cornuta* and *V. philippica*–*V. prionantha* in response to photoperiod variation may be essential for the CH–CL transition. The differential expression of the *AP3* orthologous genes among *Viola* species may be influenced by the presence and distribution of *cis*-acting elements related to light in their regulatory regions. We found similar putative promoter sequences for *AP3* orthologous genes in *V. philippica* and *V. prionantha*, but they were quite diverged from those in *V. cornuta*. Light can significantly regulate gene expression in the presence of light-responsive elements, such as Gap-boxes in the promoter [58, 59]. PHYTOCHROME A, 3AF1, and GAF1 factors can bind to the chs-CMA2a element, GA-motif, and Gap-box, respectively, and regulate target gene expression [58, 60–62]. In our study, differences in the presence and distribution of Sp1-motif, chs-CMA2a element, GA-motif, Gap-box, and LS7 element were observed between *VcoAP3*, *VphAP3*, and *VprAP3*, which might correlate to expression variations in these *AP3* orthologous genes in response to photoperiod variation. Moreover, extensive crosstalk occurs between the light and auxin signaling pathways, and light may affect auxin-responsive gene expression [63, 64]. Auxin-responsive elements bound by auxin response transcription factors (ARFs) regulate the expression of target genes and promote petal expansion, stamen development, and petal spur elongation and nectary maturation [65–68]. The changes in auxin levels and differential expression of ARFs are associated with dimorphic flower development in *Sinoswertia tetraptera* [1]. Furthermore, the photoperiod regulates the circadian clock [69], and CIRCADIAN CLOCK ASSOCIATED 1 (CCA1) regulates a variety of genes by directly binding to their promoters [70–72]. An auxin-responsive element was only found in the putative promoters of *VphAP3* and *VprAP3*, and a circadian element was only found in that of *VcoAP3*, which might also be related to the differential expression of these genes in response to photoperiod variation. In addition, introns may be involved in the regulation of gene expression [73–75]. We found that the intron regions, particularly the fourth intron of *VcoAP3*, differed from that of *VphAP3* and *VprAP3* in length and *cis*-element presence. Further functional investigation is required to identify the precise role of the observed sequence divergence of putative promoters and introns in the expression variations of these *Viola AP3* orthologous genes in response to the photoperiod. Because AP3 conservatively formed the obligate heterodimers with other B-class MADS-domain proteins, such as PI and TM6, in the studied *Viola* species, we conclude that the differential expression of *AP3* orthologous genes and the expression alteration of *PI* and *TM6* homologous genes are altogether involved in regulating the CH–CL transition in *Viola*.

Supplementary Information

The online version contains supplementary material available at https://doi.org/10.1186/s12870-025-06348-6.

Supplementary Material 1: Figs. S1–S6 in one PDF file.

Supplementary Material 2: Tables S1–S3 in one EXCEL file.

Acknowledgements

We sincerely thank the assistance of Hailong Pang (Life Science College, Northwest Normal University) in BiFC analysis. This work was supported by the grants (32160055, 32360059, and 31930007) from the National Natural Science Foundation of China.

Authors' contributions
QXL conceived and designed the work. QXL, JGL, KS, and CYH analyzed the data. QXL, YYZ, YLL, and CLC performed experiments. QXL and CYH wrote the manuscript. All authors have read and approved the manuscript.

Funding
This work was supported by the grants (32160055, 32360059, and 31930007) from the National Natural Science Foundation of China.

Data availability
All data is available in the manuscript or the supplementary materials. Sequences reported in this work have been deposited in the NCBI database, with accession numbers PQ147835–PQ147841.

Declarations

Ethics approval and consent to participate
Not applicable.

Consent for publication
Not applicable.

Competing interests
The authors declare no competing interests.

Received: 4 August 2024 Accepted: 4 March 2025
Published online: 12 March 2025

References

1. Zhu M, Wang Z, Yang Y, Wang Z, Mu W, Liu J. Multi-omics reveal differentiation and maintenance of dimorphic flowers in an alpine plant on the Qinghai-Tibet Plateau. Mol Ecol. 2023;32:1411–24.
2. Li QX, Huo QD, Wang J, Zhao J, Sun K, He CY. Expression of B-class MADS-box genes in response to variations in photoperiod is associated with chasmogamous and cleistogamous flower development in *Viola philippica*. BMC Plant Biol. 2016;6:151.
3. Li QX, Li KP, Zhang ZR, Li JG, Wang B, Zhang ZM, Zhu YY, Pan CC, Sun K, He CY. Transcriptomic comparison sheds new light on regulatory networks for dimorphic flower development in response to photoperiod in *Viola prionantha*. BMC Plant Biol. 2022;22:336.
4. Culley TM, Klooster MR. The cleistogamous breeding system: a review of its frequency, evolution, and ecology in angiosperms. Bot Rev. 2007;73:1–30.
5. Anwar N, Ohta M, Yazawa T, Sato Y, Li C, Tagiri A, Sakuma M, Nussbaumer T, Bregitzer P, Pourkheirandish M, Wu J, Komatsuda T. MiR172 downregulates the translation of *cleistogamy* 1 in barley. Ann Bot. 2018;122:251–65.
6. Lord EM. Cleistogamy: a tool for the study of floral morphogenesis, function and evolution. Bot Rev. 1981;47:421–49.
7. Minter TC, Lord EM. Effects of water stress, abscisic acid, and gibberellic acid on flower production and differentiation in the cleistogamous species *Collomia grandiflora* Dougl. ex Lindl. (Polemoniaceae). Am J Bot. 1983;70:618–24.
8. Jack T, Brockman LL, Meyerowitz EM. The homeotic gene *APETALA3* of *Arabidopsis thaliana* encodes a MADS box and is expressed in petals and stamens. Cell. 1992;68:683–97.
9. Goto K, Meyerowitz EM. Function and regulation of the *Arabidopsis* floral homeotic gene *PISTILLATA*. Genes Dev. 1994;8:1548–60.
10. Jack T, Fox GL, Meyerowitz EM. *Arabidopsis* homeotic gene *APETALA3* ectopic expression: transcriptional and posttranscriptional regulation determine floral organ identity. Cell. 1994;76:703–16.
11. Theissen G. Development of floral organ identity: stories from the MADS house. Curr Opin Plant Biol. 2001;4:75–85.
12. Immink RG, Kaufmann K, Angenent GC. The "ABC" of MADS domain protein behaviour and interactions. Semin Cell Dev Biol. 2010;21:87–93.
13. Bowman JL, Smyth DR, Meyerowitz EM. Genes directing flower development in *Arabidopsis*. Plant Cell. 1989;1:37–52.
14. Hill JP, Lord EM. Floral development in *Arabidopsis thaliana*: a comparison of the wild type and the homeotic *pistillata* mutant. Can J Bot. 1989;67:2922–36.
15. Wuest SE, O'Maoileidigha DS, Rae L, Kwasniewska K, Raganelli A, Hanczaryk K, Lohan AJ, Loftus B, Graciet E, Wellmer F. Molecular basis for the specification of floral organs by *APETALA3* and *PISTILLATA*. Proc Natl Acad Sci USA. 2012;109:13452–7.
16. Zhang R, Guo C, Zhang WG, Wang PP, Li L, Duan XS, Du QG, Zhao L, Shan HY, Hodges SA, Kramer EM, Ren Y, Kong HZ. Disruption of the petal identity gene *APETALA3-3* is highly correlated with loss of petals within the buttercup family (Ranunculaceae). Proc Natl Acad Sci USA. 2013;110:5074–9.
17. Sun JJ, Li F, Wang DH, Liu XF, Li X, Liu N, Gu HT, Zou C, Luo JC, He CX, Huang SW, Zhang XL, Xu ZH, Bai S-N. *CsAP3*: a cucumber homolog to *Arabidopsis APETALA3* with novel characteristics. Front Plant Sci. 2016;7:1181.
18. Dirks-Mulder A, Butôt R, Schaik PV, Wijnands JWPM, Berg RVD, Krol L, Doebar S, Kooperen KV, Boer HD, Kramer EM, Smets EF, Vos RA, Vrijdaghs A, Gravendeel B. Exploring the evolutionary origin of floral organs of *Erycina pusilla*, an emerging orchid model system. BMC Evol Biol. 2017;17:89.
19. Cheon KS, Nakatsuka A, Tasaki K, Kobayashi N. Long-lasting corolla cultivars in Japanese azaleas: a mutant AP3/DEF homolog identified in traditional azalea cultivars from more than 300 years ago. Front Plant Sci. 2018;8:2239.
20. Zhang Y, Liu B, Yang S, An J, Chen C, Zhang X, Ren H. A cucumber *DELLA* homolog *CsGAIP* may inhibit staminate development through transcriptional repression of B class floral homeotic genes. PLoS ONE. 2014;9: e91804.
21. Rieu P, Turchi L, Thévenon E, Zarkadas E, Nanao M, Chahtane H, Tichtinsky G, Lucas J, Blanc-Mathieu R, Zubieta C, Schoehn G, Parcy F. The F-box protein UFO controls flower development by redirecting the master transcription factor LEAFY to new *cis*-elements. Nat Plants. 2023;9:315–29.
22. Krizek BA, Bantle AT, Heflin JM, Han H, Freese NH, Loraine AE. AINTEGUMENTA and AINTEGUMENTA-LIKE6 directly regulate floral homeotic, growth, and vascular development genes in young *Arabidopsis* flowers. J Exp Bot. 2021;72:5478–93.
23. Lee JY, Baum SF, Alvarez J, Patel A, Chitwood DH, Bowman JL. Activation of *CRABS CLAW* in the nectaries and carpels of *Arabidopsis*. Plant Cell. 2005;17:25–36.
24. Lu C, Qu J, Deng C, Liu F, Zhang F, Huang H, Dai S. The transcription factor complex CmAP3-CmPI-CmUIF1 modulates carotenoid metabolism by directly regulating the carotenogenic gene *CmCCD4a-2* in chrysanthemum. Hortic Res. 2022;9:uhac020.
25. Ma Z, Yang Q, Zeng L, Li J, Jiao X, Liu Z. FaesAP3_1 regulates the *FaesELF3* gene involved in filament-length determination of long-homostyle *Fagopyrum esculentum*. Int J Mol Sci. 2022;23:14403.
26. Ito T, Wellmer F, Yu H, Das P, Ito N, Alves-Ferreira M, Riechmann J, Meyerowitz EM. The homeotic protein *AGAMOUS* controls microsporogenesis by regulation of *SPOROCYTELESS*. Nature. 2004;15:356–60.
27. Mayers AM, Lord EM. Comparative flower development in the cleistogamous species *Viola odorata*. I. A growth rate study. Am J Bot. 1983;70:1548–55.
28. Sternberger AL, Ruhil AVS, Rosenthal DM, Ballard HE, Wyatt SE. Environmental impact on the temporal production of chasmogamous and cleistogamous flowers in the mixed breeding system of *Viola pubescens*. PLoS ONE. 2020;15: e0229726.
29. Qin B, Chen QP, Lou ZC. Active constituents of *Viola prionantha* Bge. J Chin Pharm Sci. 1994;3:91–6.
30. Xie C, Kokubun T, Houghton PJ, Simmonds MS. Antibacterial activity of the Chinese Traditional Medicine, zi hua di ding. Phytother Res. 2004;18:497–500.
31. Zuo J, He H, Zuo Z, Bou-Chacra N, Lobenberg R. Erding formula in hyperuricaemia treatment: unfolding traditional Chinese herbal compatibility using modern pharmaceutical approaches. J Pharm Pharmacol. 2018;70:124–32.
32. Kramer EM, Su HJ, Wu JM, Hu JM. A simplified explanation for the frameshift mutation that created a novel C-terminal motif in the *APETALA3* gene lineage. BMC Evol Biol. 2006;6:30.
33. de Martino G, Pan I, Emmanuel E, Levy A, Irish VF. Functional analyses of two tomato *APETALA3* genes demonstrate diversification in their roles in regulating floral development. Plant Cell. 2006;18:1833–45.

34. Larkin MA, Blackshields G, Brown NP, Chenna R, McGettigan PA, McWilliam H, Valentin F, Wallace IM, Wilm A, Lopez R, Thompson JD, Gibson TJ, Higgins DG. Clustal W and Clustal X version 20. Bioinformatics. 2007;23:2947–8.
35. Jones DT, Taylor WR, Thornton JM. The rapid generation of mutation data matrices from protein sequences. Comput Appl Biosci. 1992;8:275–82.
36. Livak KJ, Schmittgen TD. Analysis of relative gene expression data using real-time quantitative PCR and the $2^{-\Delta\Delta CT}$ method. Methods. 2001;25:402–8.
37. Javelle M, Marco CF, Timmermans M. *In situ* hybridization for the precise localization of transcripts in plants. J Vis Exp. 2011;57:3328.
38. Gong PC, Zhao M, He CY. Slow co-evolution of the MAGO and Y14 protein families is required for the maintenance of their obligate heterodimerization mode. PLoS ONE. 2014;1: e84842.
39. Gong PC, Ao X, Liu GX, Cheng FY, He CY. Duplication and whorl-specific downregulation of the obligate AP3-PI heterodimer genes explain the origin of *Paeonia lactiflora* plants with spontaneous corolla mutation. Plant Cell Physiol. 2017;58:411–25.
40. Melzer R, Härter A, Rümpler F, Kim S, Soltis PS, Soltis DE, Theißen G. DEF- and GLO-like proteins may have lost most of their interaction partners during angiosperm evolution. Ann Bot. 2014;114:1431–43.
41. Clavijo ERD, Jimenez MJ. Cleistogamy and chasmogamy in *Ceratocapnos heterocarpa* (Fumariaceae). Int J Plant Sci. 1993;154:325–33.
42. Le Corff J. Effects of light and nutrient availability on chasmogamy and cleistogamy in an understory tropical herb, *Calathea micans* (Marantaceae). Am J Bot. 1993;80:1392–9.
43. Wang Y, Ballard HE, McNally RR, Wyatt SE. Gibberellins are involved but not sufficient to trigger a shift between chasmogamous-cleistogamous flower types in *Viola pubescens*. J Torrey Bot Soc. 2013;140:1–8.
44. Miranda AS, Vieira MF. Production of floral morphs in cleistogamous *Ruellia brevifolia* (Pohl) C. Ezcurra (Acanthaceae) at different levels of water availability. J Pollinat Ecol. 2016;19:104–7.
45. Kramer EM, Dorit RL, Irish VF. Molecular evolution of genes controlling petal and stamen development: duplication and divergence within the *APETALA3* and *PISTILLATA* MADS-box gene lineages. Genetics. 1998;149:765–83.
46. Irish VF. Evolution of petal identity. J Exp Bot. 2009;10:2517–27.
47. Lee HL, Irish VF. Gene duplication and loss in a MADS box gene transcription factor circuit. Mol Biol Evol. 2011;28:3367–80.
48. Zeng L, Zhang J, Wang X, Liu Z. Isolation and characterization of *APETALA3* orthologs and promoters from the distylous *Fagopyrum esculentum*. Plants. 2021;10:1644.
49. Arango-Ocampo C, González F, Alzate JF, Pabón-Mora N. The developmental and genetic bases of apetaly in *Bocconia frutescens* (Chelidonieae: Papaveraceae). EvoDevo. 2016;7:16.
50. Galimba KD, Martínez-Gómez J, Di Stilio VS. Gene duplication and transference of function in the paleoAP3 lineage of floral organ identity genes. Front Plant Sci. 2018;9:334.
51. Otani M, Aoyagi K, Nakano M. Suppression of B function by chimeric repressor gene-silencing technology (CRES-T) reduces the petaloid tepal identity in transgenic *Lilium* sp. PLoS ONE. 2020;15: e0237176.
52. Yoshida H, Itoh JI, Ohmori S, Miyoshi K, Horigome A, Uchida E, Kimizu M, Matsumura Y, Kusaba M, Satoh H, Nagato Y. *Superwoman1-cleistogamy*, a hopeful allele for gene containment in GM rice. Plant Biotech J. 2007;5:835–46.
53. Su Z, Ma X, Guo HH, Sukiran NL, Guo B, Assmann SM, Ma H. Flower development under drought stress: Morphological and transcriptomic analyses reveal acute responses and long-term acclimation in *Arabidopsis*. Plant Cell. 2013;10:3785–807.
54. Müller F, Xu J, Kristensen L, Wolters-Arts M, de Groot PFM, Jansma SY, Mariani C, Park S, Rieu I. High-temperature-induced defects in tomato (*Solanum lycopersicum*) anther and pollen development are associated with reduced expression of B-Class floral patterning genes. PLoS ONE. 2016;11: e0167614.
55. Kim ST, Koh J, Yoo MJ, Kong HZ, Hu Y, Ma H, Soltis PS, Soltis DE. Expression of floral MADS-box genes in basal angiosperms: implications for the evolution of floral regulators. Plant J. 2005;43:724–44.
56. Zhao YH, Möller M, Yang JB, Liu TS, Zhao JF, Dong LN, Zhang JP, Li CY, Wang GY, Li DZ. Extended expression of B-class MADS-box genes in the paleoherb *Asarum caudigerum*. Planta. 2010;231:265–76.
57. Kivivirta KI, Herbert D, Roessner C, de Folter S, Marsch-Martinez N, Becker A. Transcriptome analysis of gynoecium morphogenesis uncovers the chronology of gene regulatory network activity. Plant Physiol. 2021;185:1076–90.
58. Conley TR, Park S, Kwon H, Peng H, Shih M. Characterization of cis-acting elements in light regulation of the nuclear gene encoding the a subunit of chloroplast isozymes of glyceraldehyde-3-phosphate dehydrogenase from *Arabidopsis thaliana*. Mol Cell Biol. 1994;14:2525–33.
59. Qian M, Ni J, Niu Q, Bai S, Bao L, Li J, Sun Y, Zhang D, Teng Y. Response of miR156-SPL module during the red peel coloration of bagging-treated Chinese sand pear (*Pyrus pyrifolia* Nakai). Front Physiol. 2017;8:550.
60. Gilmartin PM, Sarokin L, Memelink J, Chua NH. Molecular light switches for plant genes. Plant Cell. 1990;2:369–78.
61. Lam E, Kano-Murakami Y, Gilmartin Y, Niner B, Chua NH. A metal-dependent DNA-binding protein interacts with a constitutive element of a light-responsive promote. Plant Cell. 1990;2:857–66.
62. Hudson ME, Quail PH. Identification of promoter motifs involved in the network of phytochrome A-regulated gene expression by combined analysis of genomic sequence and microarray data. Plant Physiol. 2003;133:1605–16.
63. Sibout R, Sukumar P, Hettiarachchi C, Holm M, Muday GK, Hardtke CS. Opposite root growth phenotypes of *hy5* versus *hy5 hyh* mutants correlate with increased constitutive auxin signaling. PLoS Genet. 2006;2: e202.
64. van Gelderen K, Kang C, Paalman R, Keuskamp D, Hayes S, Pierik R. Far-red light detection in the shoot regulates lateral root development through the HY5 transcription factor. Plant Cell. 2018;30:101–16.
65. Ulmasov T, Hagen G, Guilfoyle TJ. ARF1, a transcription factor that binds to auxin response elements. Science. 1997;276:1865–8.
66. Reeves PH, Ellis CM, Ploense SE, Wu M-F, Yadav V, Tholl D, Chételat A, Haupt I, Kennerley BJ, Hodgens C, Farmer EE, Nagpal P, Reed W. A regulatory network for coordinated flower maturation. PLoS Genet. 2012;8: e1002506.
67. Freire-Rios A, Tanaka K, Crespo I, van der Wijk E, Sizentsova Y, Levitsky V, Lindhoud S, Fontana M, Hohlbein J, Boer DR, Mironova V, Weijers D. Architecture of DNA elements mediating ARF transcription factor binding and auxin-responsive gene expression in *Arabidopsis*. Proc Natl Acad Sci USA. 2020;117:24557–66.
68. Zhang R, Min Y, Holappa D, Walcher-Chevillet CL, Duan XS, Donaldson E, Kong HZ, Kramer EM. A role for the auxin response factors ARF6 and ARF8 homologs in petal spur elongation and nectary maturation in *Aquilegia*. New Phytol. 2020;227:1392–405.
69. Faehn C, Reichelt M, Mithöfer A, Hytönen T, Mølmann J, Jaakola L. Acclimation of circadian rhythms in woodland strawberries (*Fragaria vesca* L.) to Arctic and mid-latitude photoperiods. BMC Plant Biol. 2023;23:483.
70. Wang ZY, Kenigsbuch D, Sun L, Harel E, Ong MS, Tobin EM. A Myb-related transcription factor is involved in the phytochrome regulation of an *Arabidopsis Lhcb* gene. Plant Cell. 1997;9:491–507.
71. Lu SX, Webb CJ, Knowles SM, Kim SH, Wang Z, Tobin EM. CCA1 and ELF3 interact in the control of hypocotyl length and flowering time in *Arabidopsis*. Plant Physiol. 2012;158:1079–88.
72. Park MJ, Kwon YJ, Gil KE, Park CM. LATE ELONGATED HYPOCOTYL regulates photoperiodic flowering via the circadian clock in *Arabidopsis*. BMC Plant Biol. 2016;16:114.
73. Rose AB. Intron-mediated regulation of gene expression. Curr Top Microbiol Immunol. 2008;326:277–90.
74. Rose AB, Carter A, Korf I, Kojima N. Intron sequences that stimulate gene expression in *Arabidopsis*. Plant Mol Biol. 2016;92:337–46.
75. Wang L, He LL, Li J, Zhao J, Li ZC, He CY. Regulatory change at *Physalis Organ Size 1* correlates to natural variation in tomatillo reproductive organ size. Nat Commun. 2014;5:4271.

Publisher's Note